The effects of Si incorporation on the microstructure and nanomechanical properties of DLC thin films

2000 J. Phys.: Condens. Matter 12 9201

(http://iopscience.iop.org/0953-8984/12/44/302)

J. Phys.: Condens. Matter **12** (2000) 9201–9213. Printed in the UK PII: S0953-8984(00)15136-7

The effects of Si incorporation on the microstructure and nanomechanical properties of DLC thin films

J F Zhao†, P Lemoine†, Z H Liu†‡, J P Quinn† and J A McLaughlin†

† NIBEC, School of Electrical and Mechanical Engineering, University of Ulster, Newtownabbey, County Antrim, BT37 0QB, Northern Ireland, UK
‡ MXT Inc., 1744 William Street, Suite 104, Montreal, Quebec H3J 1R4, Canada

E-mail: junfu@nibec-s1.nibec.ulst.ac.uk (J F Zhao)

Received 4 July 2000

Abstract. A small amount of silicon incorporation into diamond-like carbon (DLC) films prepared by plasma-enhanced chemical vapour deposition (PECVD) onto Al_2O_3:TiC substrates was studied by a combination of surface analysis and nanomechanical measurement techniques, namely XPS, Raman spectroscopy, nanoindentation and nanoscratch methods. Addition of silicon to the DLC films leads to an increase in the fraction of sp^3, as deduced from XPS analysis, and a decrease in the Raman band intensity ratio I_D/I_G. Although the coated substrates exhibit better scratch resistance and lubricity, the films as deposited are softer than the Al_2O_3:TiC substrates. Upon silicon incorporation, the mechanical and tribological properties are degraded. Wear protection of the Al_2O_3:TiC substrate by DLC coating corresponds to the competition between the reduction in friction coefficient and the softening of the films. It is suggested that, for such a PECVD process, the degradation of the mechanical properties is caused by the increased hydrogen content in the deposits when silicon is incorporated, as is shown by the increased Raman spectral background slope. These tendencies are attributable to the development of polymer-like chains, which can weaken the inter-molecular structure of the films.

1. Introduction

Diamond-like carbon (DLC) thin films, which have a unique combination of properties such as high hardness with high wear resistance [1], chemical inertness with corrosive resistance [2, 3] and low surface energy [4], have been studied in the last decade and have potential applications in many areas. However, examples of practical applications remain few because of several problems. The internal stresses are high, around 3 GPa [5], and can lead to adhesive failure or important plastic deformation of the substrate. High coefficients of friction at atmospheric ambient have also been measured. In recent years, many researchers have attempted to control the internal compressive stress and to increase wear resistance with lower coefficient of friction by incorporating other elements into DLC [6–8]. Because of the chemical similarity, silicon has been chosen as a promising element to improve the mechanical properties of DLC films. Normally the applications of silicon incorporated DLC films are limited to stress levels below approximately 1 GPa, corresponding to a 67% decrease of the internal stress [9]. The hardness and elastic modulus were reported either to increase [7, 10] or decrease [9], which depended on the silicon concentration and preparing techniques. It is also reported that the changes of mechanical properties were independent of the silicon concentration [11]. A better understanding of the doping effect requires a combination of compositional, microstructural

0953-8984/00/449201+13$30.00

and nanomechanical analyses. In this work, we report, for the first time, the results obtained on silicon-doped DLC by using XPS, Raman spectroscopy, nanoindentation and nanoscratch techniques. We confined the investigation to a small amount of silicon (<10 at.%) on the microstructure and nanomechanical properties of DLC films.

2. Experiment

2.1. Film deposition

All films used in the present study were deposited on Al_2O_3:TiC (70 wt.% Al_2O_3+30 wt.% TiC) substrates by plasma-enhanced chemical vapour deposition (PECVD). The PECVD system (Diavac, 320 PA) is composed mainly of a radio frequency (13.56 MHz) power supply with an auto-matching network and an aluminum reaction chamber fitted with a capacitively coupled parallel electrode [12]. All experiments were carried out at a dc self-bias voltage of 300 V and the ion current density used for the coatings was 6.2 μA cm^{-2}. Prior to DLC deposition, the substrates were thoroughly cleaned by wet methods, followed by 5 minute argon plasma etching in the reaction chamber. DLC films were directly deposited onto Al_2O_3:TiC substrates using a gas mixture of argon with acetylene (1:1.5). For DLC films with silicon addition, tetramethylsilane vapour (TMS, purity >99.9%) was introduced into the chamber during DLC deposition as a silicon precursor with a vapour flow rate varying between 1 and 6 sccm min^{-1}. The total pressure in the chamber was from 5 mTorr to 10 mTorr, which changed with the flow rate of TMS. The films examined in this work were 100 nm thick.

2.2. XPS analysis

The carbon and silicon bonding configuration and composition of the DLC films were determined by x-ray photoelectron spectroscopy (XPS). The analysis was performed on the samples using a XSAM800 (Kratos) system with a hemispherical energy analyser. A non-monochromatic Mg Kα x-ray (1253.6 eV) was used as the excitation source operated at 13 kV and with an anode current 18 mA. The residual pressure of the system was 10^{-7}–10^{-8} Pa. The samples were flooded with the secondary electrons from an auxiliary electron gun to compensate for charging effects.

2.3. Raman spectroscopy

To identify the microstructure of the films, a XY-confocal micro-Raman spectroscope (Instruments SA Labram) was used. A 25 mW argon ion laser (λ = 514.5 nm) was focused onto the samples with a highly stabilized microscope objective (magnification = 100×). To avoid thermal deterioration of the samples, a 25% neutral density filter was used. The Raman spectra were acquired using a micro-confocal hole of 400 μm in diameter, a grating with 1800 lines mm^{-1} and a spectral slit 200 μm in width. The spectra were scanned in the range of 600–2100 cm^{-1}. The total acquisition time for each spectrum was 30 seconds. A Gaussian function was used to fit the spectra resulting in a series of Raman parameters varying with the silicon concentration in the films.

2.4. Nanoindentation and nanoscratch measurements

Indentation tests were performed using a Nanoindenter XP (Nano Instruments Inc.) with a high resolution DCM (Dynamical Contact Module) head. The DCM head permits an accurate control of load and displacement for shallow indentations (1 nN load resolution

Table 1. Atomic concentration of carbon, silicon and oxygen atoms in the films obtained from XPS analysis. The coatings were co-deposited with different amounts of silicon addition by varying a TMS flow from 1 to 6 sccm min^{-1}. The binding energy (E_b), the full width at half maximum (FWMH) of the C 1s peak and the sp^3/sp^2 ratio were obtained from spectral deconvolution.

Atomic conc. (at.%)			Binding energy (eV)/FWHM (eV) of C 1s				Fraction ratio
C	Si	O	C–Si	C=C	C–C	C–O	sp^3/sp^2
94.03	0.00	5.97	—	284.8 ± 0.1 /1.4 ± 0.15	285.7 ± 0.1 /1.6 ± 0.02	287.1 ± 0.3 /1.6 ± 0.28	0.27
92.92	0.18	6.90	not detected	284.9 ± 0.1 /1.3 ± 0.15	285.7 ± 0.1 /1.7 ± 0.02	287.3 ± 0.3 /1.9 ± 0.10	0.38
89.12	1.79	9.09	284.1 ± 0.2 /1.5 ± 0.05	284.9 ± 0.2 /1.4 ± 0.05	285.8 ± 0.1 /1.4 ± 0.15	287.5 ± 0.2 /2.0 ± 0.05	0.48
86.16	3.64	10.20	283.9 ± 0.2 /1.4 ± 0.04	284.9 ± 0.1 /1.2 ± 0.14	285.7 ± 0.1 /1.4 ± 0.08	286.9 ± 0.5 /2.0 ± 0.04	0.55
85.09	5.06	9.85	284.0 ± 0.2 /1.5 ± 0.10	284.8 ± 0.1 /1.3 ± 0.12	285.5 ± 0.2 /1.5 ± 0.07	286.7 ± 0.4 /1.9 ± 0.05	0.58
83.30	7.54	9.16	284.2 ± 0.2 /1.4 ± 0.08	284.9 ± 0.1 /1.2 ± 0.14	285.7 ± 0.2 /1.4 ± 0.11	286.9 ± 0.3 /1.8 ± 0.12	0.73
79.61	9.32	11.07	284.3 ± 0.1 /1.5 ± 0.12	284.9 ± 0.1 /1.2 ± 0.12	285.8 ± 0.1 /1.1 ± 0.15	286.9 ± 0.3 /1.7 ± 0.21	0.85

for thin film test). The tests were depth control up to 60 nm and the hardness (H) and Young modulus (E) were then derived from the stiffness–unloading data by numerical fitting. Only 90% of the experimental data was used for the calculation. The results presented in the text were averaged over six indentations for each sample. The nanoscratch test was carried out under a constant load of 3 mN over 120 μm on the sample surface. The non-scratch profiles (pre-scratch and post-scratch) were acquired at 0.02 mN load. The scratch resistance was calculated by integrating the residual depth over the scratch segment.

3. Results and discussion

3.1. Effect on sp^2 and sp^3 fractions in DLC films

The XPS survey scan of the silicon-doped DLC films shows clearly the contributions from C 1s (∼285 eV), Si 2p (∼100 eV), Si 2s (∼151 eV) and O 1s (∼531 eV). Typical spectra shown in figure 1 correspond respectively to (a) without silicon and (b) with silicon incorporation. The atomic concentrations of Si, C and O elements obtained by XPS analysis are given in table 1. Figure 2 shows the correlation between TMS flow rate and the silicon (solid line)/carbon (dashed line) atomic concentrations. With increasing TMS flow rate, the silicon content is increased to 9.32 at.% at a flow rate of 6 sccm min^{-1} while the carbon content is dropped to 79.61 at.%. Compared to the XPS data obtained from a graphite surface (full width at half maximum (FWHM) = 0.6 eV) and a diamond surface (FWHM = 1.0 eV) [13], the C 1s peaks obtained in this study are broad (FWHM $\sim 1.6 \pm 0.1$ eV). This implies possible contributions from differently bonded carbons to the C 1s peak observed. In fact, deconvolution of spectra has shown that the broad C 1s peaks are composed of four peaks corresponding respectively to C–Si, C=C, C–C and C–O bonding configurations. The deconvolution of XPS spectra was done by using the Kratos software system with a Gaussian distribution function. The results are listed in table 1. In general, as an example of Voigt line shape function, a

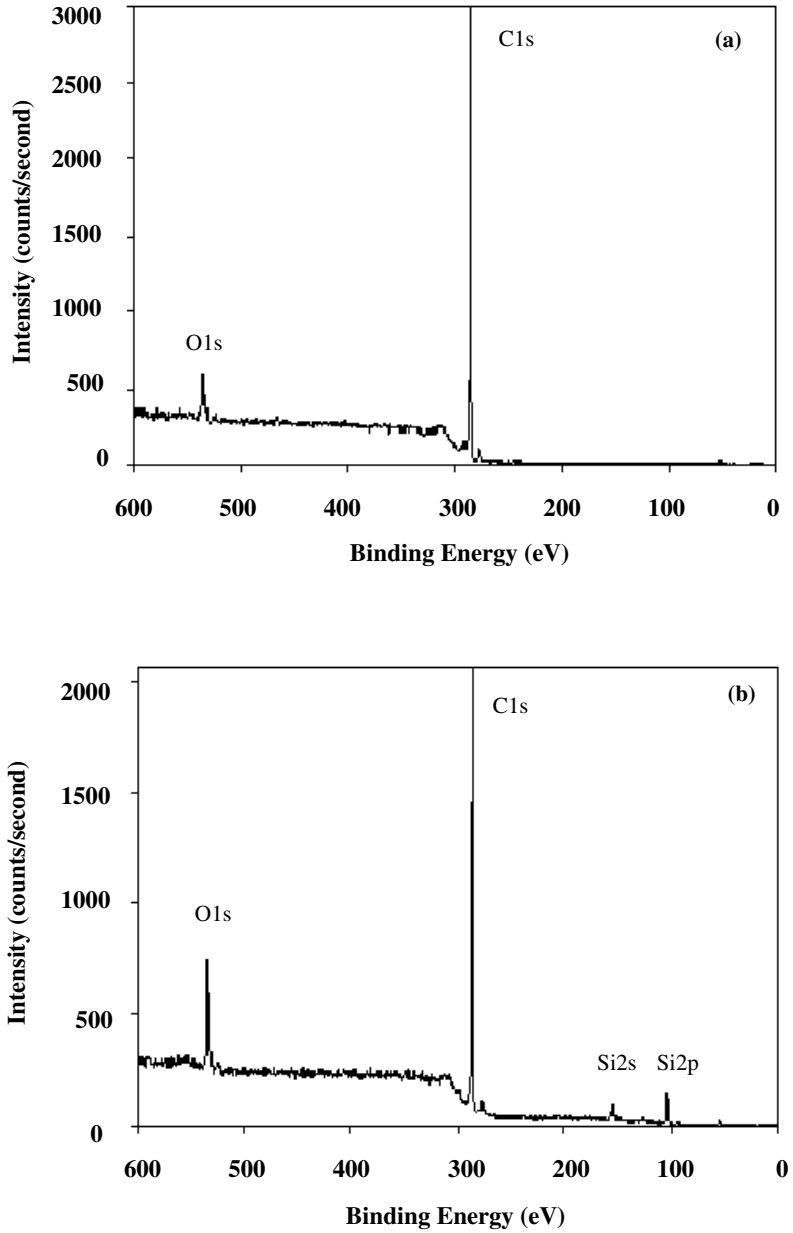

Figure 1. The survey scan XPS spectra of the DLC films deposited on Al_2O_3:TiC substrates (a) without and (b) with silicon addition.

mixed Gaussian and Lorentzian function is used to fit XPS C 1s peak to get more consistent results. In the case described here, however, it was noticed that the results obtained by using a pure Gaussian function and a mixed Gaussian with Lorentzian function are very consistent with each other. The difference in binding energy obtained by using two different types of function is less than 0.1 eV, which is within the error range given in table 1. The four peaks are well separated by 0.7–1.2 eV and are positioned respectively at 284.1 $\pm$ 0.2 eV (C–Si),

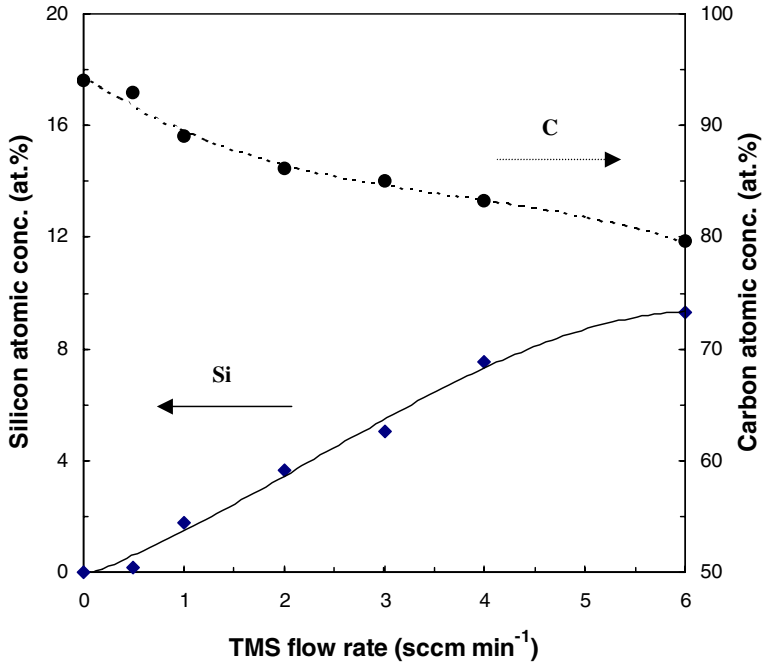

Figure 2. The TMS flow-rate-dependent silicon (solid line) and carbon (dashed line) contents in the deposits as deduced from XPS analysis.

284.8 ± 0.1 eV (C=C), 285.7 ± 0.1 eV (C–C) and 287.0 ± 0.3 eV (C–O). The FWHM of these peaks was considered to be ∼1.4–1.5 eV (C–Si), ∼1.2–1.4 eV (C=C), ∼1.4–1.7 eV (C–C) and ∼1.6–2.0 eV (C–O). The low intensity peak at ∼287.0 eV assigned to the C–O bond normally comes either from the surface contamination due to air exposure or from the use of TMS gas during deposition. The carbon double bond C=C appearing at ∼284.8 eV can be assigned to the sp^2 bonding configuration in the films. The sp^3 component can be positioned at the lower binding energy ∼284.1 eV for the C–Si bonds, or at the higher binding energy around 285.7 eV for the C–C and/or C–H bonds. Since acetylene was used as a precursor gas, the DLC deposited in this way is usually hydrogenated to some extent. In other words, the XPS peak located at 285.7 eV is attributed to both C–C and C–H bonds. Unfortunately, the hydrogen content in the samples is unknown presently and it should be analysed in future work. Therefore, it is impossible to estimate the contribution of C–H to the observed XPS peak. Thus, the sp^3/sp^2 ratio can be evaluated by the integrated areas of these bands. As expected and well demonstrated in figure 3, increasing silicon content in the deposit will increase the sp^3 fraction. For example, the C 1s peak of the undoped DLC film shows no contribution from carbon bonded to silicon (figure 3(a)). However, when silicon is co-deposited into DLC films, the contribution from silicon-bonded carbon to the C 1s peak appears at ∼284.1 eV and increases with silicon (figures 3(b)–(d)). The sp^3/sp^2 ratio as calculated is in the range of 0.27 for the DLC films without silicon and 0.85 for those with 9.32 at.% silicon. Since the structure of DLC films is extremely complex as carbon atoms can form bonds with three different types of hybridization, the properties of DLC films are largely determined by the relative proportion of sp^3 and sp^2 components in the films. Therefore, as an alternative to other techniques, such as electron energy loss spectroscopy (EELS) [14] and nuclear magnetic resonance (NMR) [15], XPS can be used to estimate the contents of sp^3

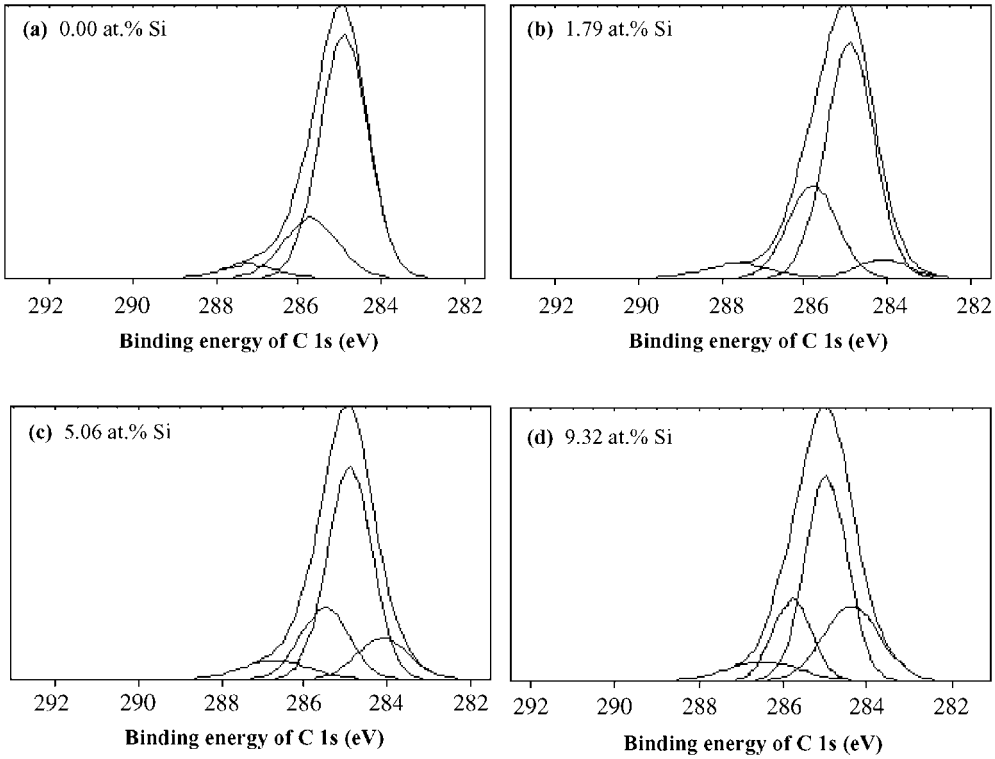

Figure 3. Deconvolution of the XPS spectra in the C 1s peak region acquired on the DLC films prepared without and with different silicon contents in the deposits.

and sp^2 fractions. Indeed, it has been applied recently to both hydrogenated and nitrogenated carbon films [15–18]. However, one must note that XPS analysis gives no information on hydrogen content and the information of these bond ratio from XPS analysis should really be complimented by EELS measurements. Nevertheless, the estimation of sp^3/sp^2 ratio is helpful to understand the effects of silicon incorporation on the microstructure and the nanomechanical properties of DLC films.

The binding energies for Si 2p and Si 2s are shown in figure 4. For most silicon contents, these binding energies are stabilized at around 103 eV (Si 2p) and 154 eV (Si 2s), respectively. For low silicon content in deposits, the binding energy of the Si 2p peak falls below 103 eV because of the presence of some Si–H bonds. It is also possible that the existence of Si–O bonds could appear between 103 eV and 104 eV [19]. The FWHM of the Si 2p peak is in the range of 1.4–1.6 eV except for silicon content below 1.0 at.%. The FWHM of the Si 2s peak is increased from 0.12 eV to 1.91 eV with increasing silicon concentration. The increase in the Si 2s peak width could be caused by silicon atoms bonded to carbon atoms in different hybridization states of sp^2 and sp^3.

Since XPS is a very surface sensitive technique, the detection of oxygen suggests various sources of surface contamination. The oxygen detected in the films prepared without TMS introduction into the chamber during deposition (see figure 1(a)) corresponds to contamination from post-deposition, i.e. from air exposure. It was also found that the oxygen signal increases with TMS flow rate, implying that this type of contamination was enhanced by using TMS. Oxygen atoms might more easily attach to silicon than to carbon as bridging or non-bridging

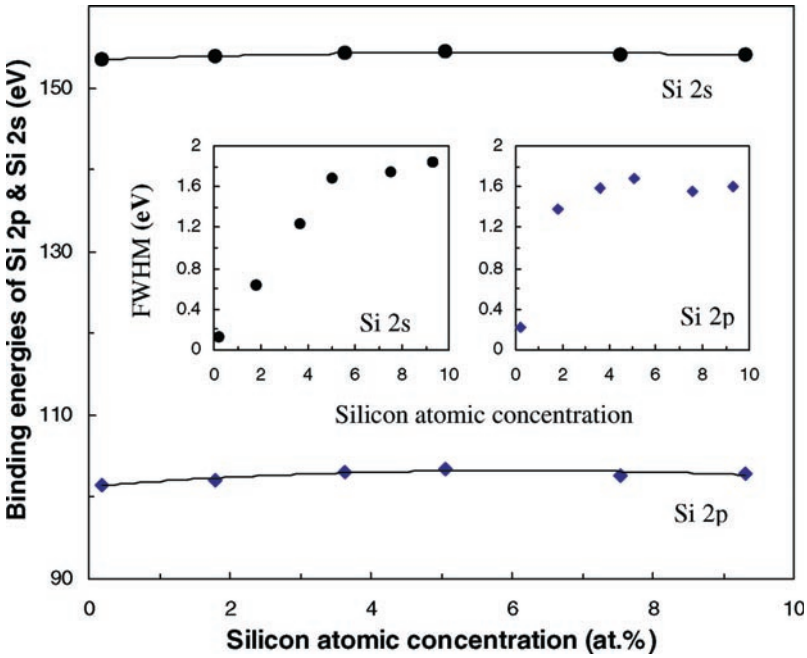

Figure 4. The binding energy and the full width at half maximum (FWHM) of Si 2p and Si 2s peaks as a function of silicon content in the DLC films.

species, leading to an increase in the band intensity and shifting up the binding energy of O 1s to ∼534 eV, with an FWHM of ∼2.0 eV.

3.2. Effect on microstructure of the films

Figure 5 shows the effect of silicon concentration on the Raman spectra of DLC films. The addition of silicon atoms seems to decrease the asymmetry of the Raman peak. Comparing figures 5(b) and (c), the Raman spectrum of DLC films without silicon shows a broad asymmetric band centred around 1543 cm^{-1} with a total FWHM of 176 cm^{-1}. However, for DLC films with silicon, this broad band is shifted to 1497 cm^{-1} with a total FWHM of 128 cm^{-1}. The reduction in FWHM indicates that the shoulder becomes smaller and the peak is thus more symmetrical. To interpret the Raman spectra of amorphous carbon materials, the peak is usually deconvoluted into two peaks called the D band and G band. The D band corresponds to the disordering of the activated optic zone edge phonons in the vibrational density of states of layered sp^2 structures [20, 21]. The G band positioned at the higher frequency side is attributed to a decrease in the C–C stretching vibration resulting from the lengthening of the C–C bond. The corresponding Raman parameters are listed in table 2. Figure 6 gives (a) the intensity ratio I_D/I_G of D to G band and (b) the G (solid line) and D (dashed line) band positions as a function of silicon concentration. Three features can be identified with increasing silicon concentration: (1) the Raman D and G band positions are shifted to lower frequencies; (2) the intensity ratio I_D/I_G decreases; (3) the Raman line shape changes from asymmetric to more symmetric. The data given in figure 6(b) show that the D and G band positions have been reduced respectively from 1354 and 1543 cm^{-1} for undoped DLC films to 1318 and 1497 cm^{-1} for DLC films with 9.32 at.% silicon. On the one

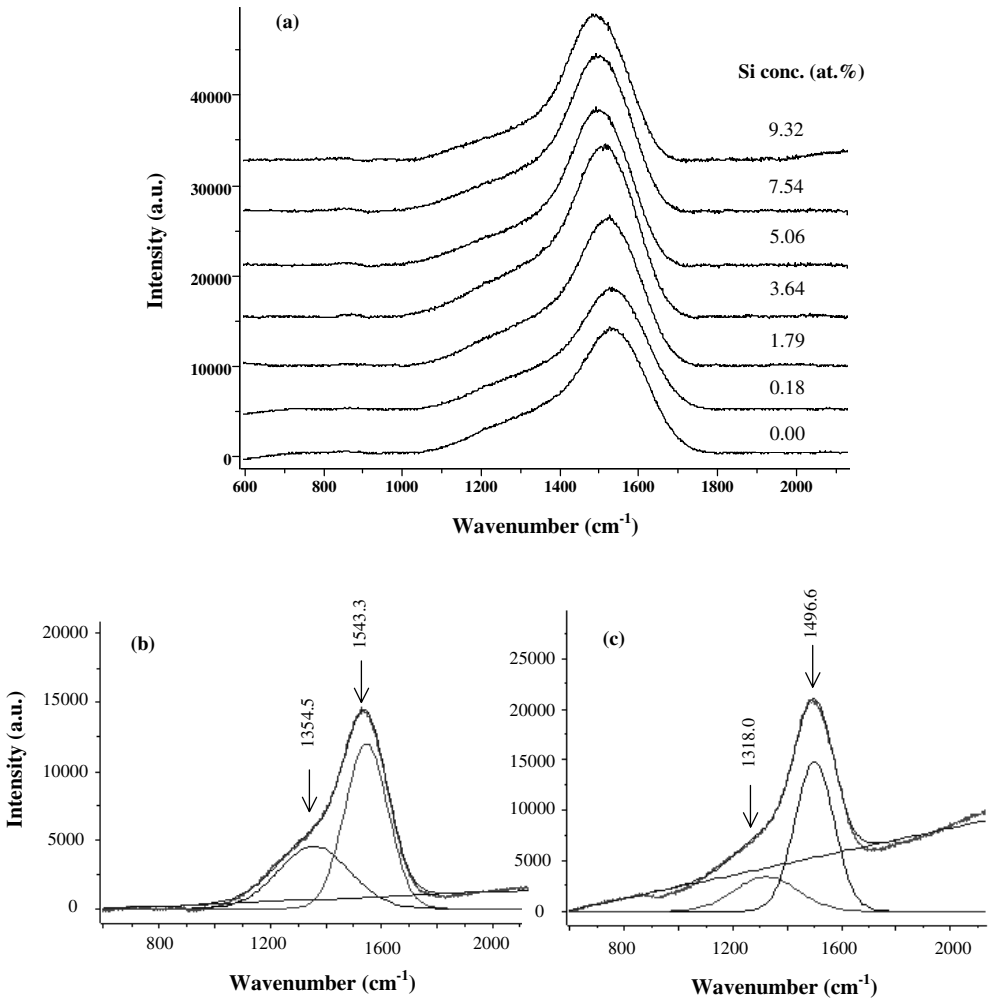

Figure 5. (a) Raman spectra of DLC films deposited on Al_2O_3:TiC substrates with different silicon addition. Also shown herein are (b) typical fitted Raman spectra for pure DLC and (c) for the DLC film with a 9.32 at.% Si addition.

hand, the shift of the G band position to a lower frequency can be partially attributed to the reduction of compressive stress when silicon is introduced into the films because the longer de-strained bonds vibrate at the lower frequencies [9]. The presence of Si–C bridging bonds can weaken the adjacent C–C bonds resulting in a downward frequency shift of the D and G bands. On the other hand, the frequency shift can also be accounted for by the disordering of sp^2-bonded clusters as reported elsewhere [22]. Similarly, the decrease of intensity ratio I_D/I_G is due to the change in stress and/or the change in crystallite size of sp^2-bonded clusters [22–24]. The structure of silicon incorporated DLC films is extremely complex with a varied amount of threefold- and fourfold-coordinated carbon and silicon bondings in the DLC matrix. Clustering of similarly bonded carbon atoms can also provide very little or a large quantity of hydrogen atoms [25]. Therefore, it is not always easy to predict the effect on Raman intensity ratios. However, considering that the films formed by the PECVD method are all amorphous

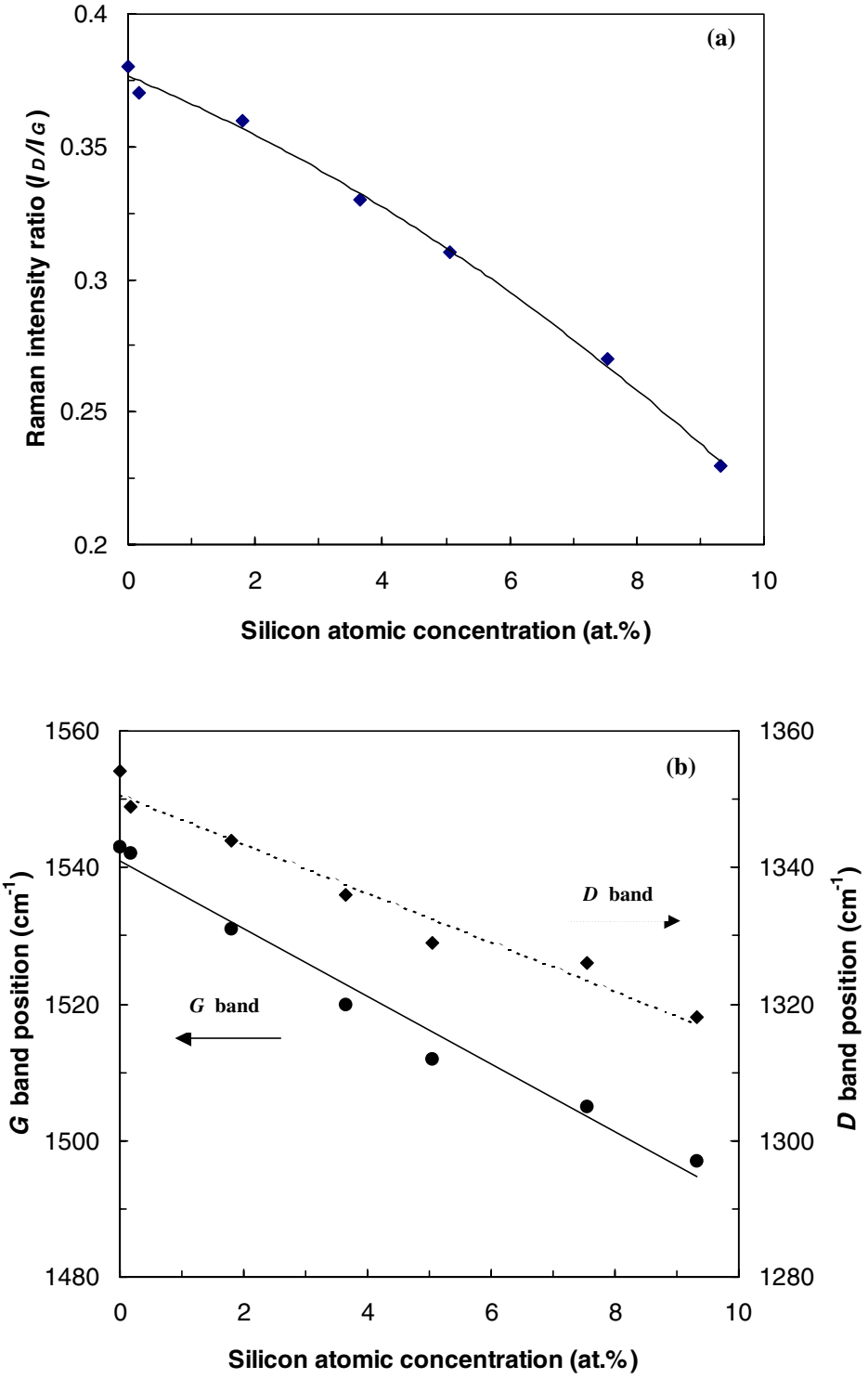

Figure 6. The silicon-concentration-dependent (a) Raman intensity ratio I_D/I_G and (b) G band (solid line) and D band (dashed line) positions for DLC films deposited on Al_2O_3:TiC substrates.

Table 2. The Raman parameters obtained by spectral fitting for the DLC films deposited onto Al_2O_3:TiC substrates with varying amount of silicon addition.

Si conc. (at.%)	Band position (cm^{-1}) D	Band position (cm^{-1}) G	Band intensity (a.u.) D	Band intensity (a.u.) G	FWHM (cm^{-1}) D	FWHM (cm^{-1}) G	Intensity ratio I_D/I_G	Background line slope k
0.00	1354 ± 3.2	1543 ± 2.0	4567 ± 10.2	$12\,024 \pm 30.1$	181 ± 3.8	111 ± 1.2	0.38	0.89
0.18	1347 ± 2.5	1543 ± 2.7	4374 ± 18.5	$11\,761 \pm 52.1$	185 ± 5.2	111 ± 3.1	0.37	0.87
1.79	1344 ± 1.2	1531 ± 3.7	5124 ± 30.1	$14\,398 \pm 19.8$	184 ± 2.4	107 ± 1.2	0.36	1.78
3.64	1336 ± 2.1	1520 ± 2.5	5590 ± 25.9	$16\,824 \pm 34.1$	178 ± 3.3	105 ± 2.1	0.33	2.86
5.06	1329 ± 3.3	1512 ± 4.6	5904 ± 13.5	$19\,040 \pm 20.4$	178 ± 4.2	104 ± 1.3	0.31	3.60
7.54	1326 ± 4.2	1505 ± 5.2	4184 ± 20.1	$15\,545 \pm 54.7$	168 ± 2.1	102 ± 5.7	0.27	4.43
9.32	1318 ± 3.0	1497 ± 4.5	3405 ± 21.7	$14\,771 \pm 30.5$	160 ± 5.7	102 ± 3.2	0.23	5.82

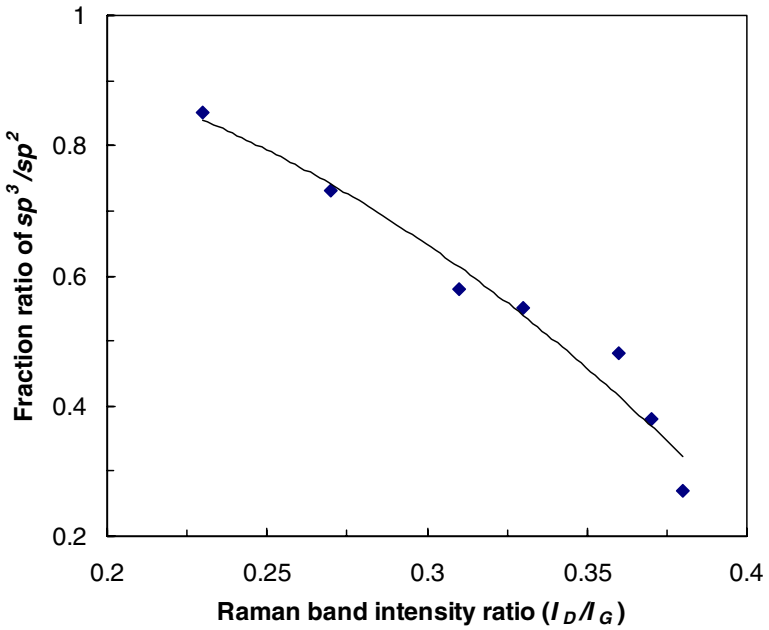

Figure 7. The relationship between Raman band intensity ratio I_D/I_G and the bond fraction ratio of sp^3/sp^2 obtained from Raman and XPS analyses for the DLC films with different silicon contents.

network structures, the effect of cluster size can be ignored. Thus, the structure network is mainly influenced by the change in the stress state of the films. Moreover, the interpretation of the microstructure is complicated by the addition of silicon into the film. For instance, the increase in the sp^3 component, as obtained from XPS analysis, could reflect silicon valence structure, which is well known to show only sp^3 hybridization.

Figure 7 gives the correlation between the bond fraction ratio sp^3/sp^2, as deduced from XPS analysis, and the Raman band intensity ratio I_D/I_G for the DLC films without and with silicon incorporation. Therefore, the decrease in band intensity ratio implies that the amount of sp^2-bonded carbon clusters decreases, accompanying an increase of mixed sp^3-bonded carbon and silicon clusters. This is consistent with the results reported by Lee *et al* [7] and indicates that the microstructure of DLC can be modified by silicon incorporation into the film.

Table 3. Hardness (H), Young's modulus (E) and scratch data obtained on uncoated and DLC-coated Al_2O_3:TiC substrates. The coatings were co-deposited with different amounts of silicon addition. The H and E values were calculated based on the depth-controlled test data up to 60 nm. The residual depth corresponds to the plastic deformation produced during scratch test under a constant load of 3 mN.

Samples	Si conc. (at.%)	Young's modulus E (GPa)	Hardness H (GPa)	Residual depth (nm)
Al_2O_3:TiC	—	473.84 ± 58.4	28.40 ± 1.8	22.71 ± 1.8
DLC	0.00	272.86 ± 10.9	24.89 ± 2.1	12.67 ± 0.9
Si-DLC	0.18	299.89 ± 15.9	24.63 ± 1.9	14.19 ± 1.1
Si-DLC	1.79	244.39 ± 22.6	18.85 ± 0.8	17.79 ± 0.9
Si-DLC	3.64	224.27 ± 6.2	14.62 ± 1.6	26.06 ± 1.1
Si-DLC	5.06	223.11 ± 12.0	14.33 ± 0.8	27.54 ± 1.0
Si-DLC	7.54	222.86 ± 17.2	14.80 ± 0.3	28.05 ± 0.6
Si-DLC	9.32	192.73 ± 3.0	13.27 ± 1.3	29.67 ± 0.9

3.3. Effect on nanomechanical properties of the films

To assess the quality of a film to be used as a wear protective layer, it is important to characterize their mechanical properties such as hardness (H), Young's modulus (E), coefficient of friction (μ) and scratch resistance. The H and E values listed in table 3 were calculated for a depth-controlled test up to 60 nm, which corresponds to a load of 0.95–1.80 mN. The scratch tests were performed with a much broader Berkovitch tip than in the indentation test. Hence a large load was used in the scratch test.

Table 3 shows that the hardness H and Young's modulus E of the films are always smaller than those of the Al_2O_3:TiC substrate. However, the measurement of scratch residual depths showed that, up to 1.79 at.% Si incorporation, the DLC films exhibit a better scratch resistance than the Al_2O_3:TiC substrate. With increasing silicon concentration, the mechanical properties of the films are degraded. For example: $H = 24.89 \pm 2.1$ GPa and $E = 272.86 \pm 10.9$ GPa for DLC films without silicon addition, $H = 13.27 \pm 1.3$ GPa and $E = 192.73 \pm 3.0$ GPa for DLC films with 9.32 at.% silicon. The scratch resistance is further lowered when more silicon atoms are incorporated into the films. The residual depths increase from 12.67 nm to 29.67 nm for DLC films without and with 9.32 at.% silicon addition, respectively. For all samples, the total deformation during scratch (<68 nm) was well within the film thickness. This means that the nanoscratch tests actually probe the mechanical properties of the films. Therefore, the scratch progresses essentially go through ploughing of the film rather than film/substrate delamination or substrate plasticization. The coefficient of friction (μ) of the films measured during the scratch segment did not show any trend with silicon incorporation. In this case, film failure by ploughing is consistent with the parallel decrease of H and E on the one hand, and the scratch resistance on the other hand. Generally, the films exhibit lower coefficient of friction than the Al_2O_3:TiC substrate (0.38 for the substrate and 0.18–0.22 for the films). The wear protection of the Al_2O_3:TiC substrate probably corresponds to a balance between the reduction in friction and the softening of the films caused by silicon incorporation.

Now, it is necessary to compare the nano-mechanical results with the structural and bonding information derived from XPS and Raman data. The spectroscopic results show an increase in the sp^3/sp^2 ratio and a decrease in the Raman intensity ratio I_D/I_G, which are usually associated with an improvement of the mechanical and wear properties of amorphous carbon films. This is clearly not the case for the present study. This apparent contradiction can be lifted if one considers that films prepared at room temperature using a PECVD technique are

likely to be saturated by hydrogen atoms, especially when using a TMS precursor. Hydrogen atoms are bonded not only to carbon but also to silicon. Since C–H bonds (338.49 kJ mol^{-1}) are more stable than Si–H bonds (298.74 kJ mol^{-1}), carbon atoms are expected to be more hydrogenated than silicon atoms. However, the different electronegativities of silicon (1.74) and carbon (2.50) lead to Si–H bonds being strengthened and C–H weakened if a silicon atom is bonded to a carbon atom. In any case, the presence of hydrogen is usually associated with the development of polymer-like chains. Upon silicon incorporation, these polymeric structures could develop and weaken the structural and mechanical properties of the films. Some researchers have already suggested that the hydrogen content in the carbon films can be reflected by the slope of Raman spectrum background [26], since the intensity of the photoluminescence tends to increase with increasing hydrogen content in the films [27, 28]. Indeed, the Raman spectra shown in figure 5 are superimposed on the rising flank of a broad luminescence background. The data in table 2 indicate that, with a 9.32 at.% Si addition, the slope is increased from 0.89 to 5.82, suggesting that the silicon incorporation results in a highly hydrogenated DLC film. Another possible contribution is the presence of weak Si–C bridging bonds. However, no obvious peaks related to the typical stretching vibration of covalent Si–C bonds were observed in the Raman spectra, probably because of its low content in the deposit. In this regard, Si–C bridging would further weaken the structural integrity of the DLC films. Therefore, although the incorporation of silicon atoms into DLC can increase and stabilize the tetrahedral bonding (sp^3 bonding), it can also induce the development of a polymeric structure, which will reduce the hardness and scratch resistance of the film [29]. Some intra-molecular bonds like sp^3 can be strengthened while the overall inter-molecular structure is weakened. Obviously, to take full advantage of the added lubricity and stress reduction offered by silicon incorporation, more work is required to complement the results presented herein, i.e. the investigation of the valence band spectra by XPS and the quantitative analysis of hydrogen content using EELS and other techniques.

4. Conclusions

Thin films of silicon-incorporated DLC were prepared by PECVD technique onto Al_2O_3:TiC substrates. A small amount of silicon incorporation into the films was studied by a combination of surface analyses and nanomechanical measurements. The content of silicon in the deposit varies between 0 and 9.32 at.%. The microstructures of the films were analysed by XPS and Raman spectroscopy. Nanomechanical properties, in terms of hardness, elastic modulus and nanoscratch resistance, were measured on samples with 100 nm thick deposit. Deconvolution of the XPS spectra revealed that the C 1s peak is composed of four peaks related respectively to the contributions from C–Si ($\sim$284.1$\pm$0.2 eV), C=C ($\sim$284.8$\pm$0.1 eV), C–C ($\sim$285.7$\pm$0.1 eV) and C–O ($\sim$287.0 $\pm$ 0.3 eV) bonds. Accordingly, the ratio of sp^3 to sp^2 was evaluated. Upon 9.32 at.% Si incorporation, the sp^3/sp^2 ratio has been increased from 0.27 to 0.85, while the corresponding Raman intensity ratio I_D/I_G has been decreased from 0.38 to 0.23. The hardness and Young's modulus have been decreased from 24.89 $\pm$ 2.1 GPa and 272.86 $\pm$ 10.9 GPa to 13.27 $\pm$ 1.3 GPa and 192.73 $\pm$ 3.0 GPa, respectively. The nanoscratch data also show a reduction in scratch resistance due to silicon incorporation. The changes observed in spectral parameters are consistent with the degradation of the nanomechanical properties of the films. It is concluded that increasing sp^3 bonding by silicon incorporation into a DLC film does not improve the hardness and scratch resistance of the deposit due to the increased hydrogen content in the deposit, which can weaken the inter-molecular structure and, hence, the observed changes in the nanomechanical properties.

Acknowledgments

The project is supported by Seagate Technology (Ireland) Ltd and the Industrial Research and Technology Unit of Northern Ireland. The authors would like to thank Dr D A Zeze from the University of Ulster at Coleraine for his assistance with XPS measurements and Dr B Meenan for his helpful discussion about XPS results.

References

[1] Robertson J 1992 *Diamond Relat. Mater.* **1** 397
[2] Liu Z H, Lemoine P, Zhao J F, Zhou D M, McAda E T and McLaughlin J A 1998 *Diamond Relat. Mater.* **7** 1059
[3] Liu Z H, Zhao J F and McLaughlin J A 1999 *Diamond Relat. Mater.* **8** 56
[4] Grill A and Patel V 1993 *Diamond Relat. Mater.* **2** 597
[5] Dekempeneer E H A, Jacobs R, Smeets J, Menever J, Eersels L, Blanpain B, Roos J and Oostra D J 1992 *Thin Solid Films* **217** 56
[6] Grischke M, Bewilogua K, Trojan K and Dimigen H 1995 *Surf. Coat. Technol.* **74/75** 739
[7] Lee K R, Kim M G, Cho S J, Eun K Y and Seong T Y 1997 *Thin Solid Films* **308/309** 263
[8] Wang M, Schmidt K, Reichelt K, Dimigen H and Hubsch H 1992 *J. Mater. Res.* **7** 667
[9] Meneve J, Dekempeneer E and Smeets J 1994 *Diamond Films Tech.* **4** 23
[10] Miyake S, Kaneko R, Kikuya Y and Sugimoto I 1991 *Trans. ASME J. Tribol.* **113** 384
[11] Oguri K and Arai T 1991 *Surf. Coat. Technol.* **47** 710
[12] Lamberton R W, Zhao J F, McLaughlin J A and Maguire P D 1998 *Diamond Relat. Mater.* **7** 1054
[13] Merel P, Tabbal M, Chaker M, Moisa S and Margot J 1998 *Appl. Surf. Sci.* **136** 105
[14] McNamara K M, Gleason K K, Vestyck D J and Butler J E 1992 *Diamond Relat. Mater.* **1** 1145
[15] Mobner C, Grant P, Tran H, Clarke G, Lockwood D J, Labbe H J, Mason B and Sproule I 1998 *Thin Solid Films* **317** 397
[16] Prawer S, Nugent K W, Lifshitz Y, Lemper G D, Grossman E, Kulik J, Avigal I and Kalish R 1996 *Diamond Relat. Mater.* **5** 433
[17] Jackson S T and Nuzzo R G 1995 *Appl. Surf. Sci.* **90** 195
[18] Bhattacharyya S, Hong J and Turban G 1998 *J. Appl. Phys.* **83** 3917
[19] Moulder J F, Stickle W F, Sobol P E and Bomben K D 1992 *Handbook of X-ray Photoelectron Spectroscopy* ed J Chastain (Perkin-Elmer) p 256
[20] Dillon R O, Woollam J A and Katkanant V 1984 *Phys. Rev.* B **29** 3482
[21] Richter A, Scheibe H J, Pompe W, Brzezinka K W and Muhling I 1986 *J. Non-Cryst. Solids* **88** 131
[22] Liu E, Shi X, Tay B K, Cheah L K, Tan H S, Shi J R and Sun Z 1999 *J. Appl. Phys.* **86** 6078
[23] McCulloch D G, Prawer S and Hoffman A 1994 *Phys. Rev.* B **50** 5905
[24] McCulloch D G and Prawer S 1995 *J. Appl. Phys.* **78** 3040
[25] Tallant D R, Parmeter J E, Siegal M P and Simpson R L 1995 *Diamond Relat. Mater.* **4** 191
[26] Marchon B, Gui J, Grannen K, Rauch G C, Ager J W, Silva S R P and Robertson J 1997 *IEEE Trans. Magn.* **33** 3148
[27] Yoshikawa M, Katagiri G, Ishida H, Ishitani A and Akamatsu T 1988 *J. Appl. Phys.* **64** 6464
[28] Zhao J F, Liu Z H and McLaughlin J A 1999 *Thin Solid Films* **357** 159
[29] Rubin M, Hooper C B, Cho N H and Bhushan B 1990 *J. Mater. Res.* **5** 2538